Available online at www.sciencedirect.com
ScienceDirect
Protein Expression and Purification 50 (2006) 215–222
Protein Expression & Purification
www.elsevier.com/locate/yprep

The molybdate-binding protein (ModA) of the plant pathogen *Xanthomonas axonopodis* pv. *citri*

Andrea Balan [a,*], Carolina P. Santacruz [a], Alexandre Moutran [a], Rita C.C. Ferreira [a], Francisco J. Medrano [b], Carlos A. Pérez [b], Carlos H.I. Ramos [b], Luís C.S. Ferreira [a]

[a] *Department of Microbiology, Biomedical Sciences Institute, University of São Paulo, São Paulo, SP 05008-900, Brazil*
[b] *National Laboratory of Synchrotron Light, Structural and Molecular Biology Center, Campinas, SP 13084-971, Brazil*

Received 27 April 2006, and in revised form 13 June 2006
Available onilne 27 June 2006

Abstract

The *modABC* operon of phytopathogen *Xanthomonas axonopodis* pv. *citri* (*X. citri*) encodes a putative ABC transporter involved in the uptake of the molybdate and tungstate anions. Sequence analyses showed high similarity values of ModA orthologs found in *X. campestris* pv. *campestris* (*X. campestris*) and *Escherichia coli*. The *X. citri modA* gene was cloned in pET28a and the recombinant protein, expressed in the *E. coli* BL21 (DE3) strain, purified by immobilized metal affinity chromatography. The purified protein remained soluble and specifically bound molybdate and tungstate with K_d 0.29 ± 0.12 μM and 0.58 ± 0.14 μM, respectively. Additionally binding of molybdate drastically enhanced the thermal stability of the recombinant ModA as compared to the apoprotein. This is the first characterization of a ModA ortholog expressed by a phytopathogen and represents an important tool for functional, biochemical and structural analyses of molybdate transport in *Xanthomonas* species.

Keywords: *Xanthomonas axonopodis* pv. *citri*; Molybdate; ABC transporters; Molybdate-binding protein; ModA

Although representing a rare trace element, molybdenum is required in several metabolic processes and virtually all of the biosphere nitrogen cycling relies on the activity of bacterial molybdoenzymes [1,2]. Molybdoenzymes participate in different redox reactions, including anaerobic respiration, nitrogen fixation from dinitrogen gas, and reduction of nitrate to nitrite [3,4]. Tungsten shares similar physicochemical and biological properties with molybdenum and, among some archaea and hyperthermophilic bacterial species, may replace molybdenum as an enzyme cofactor [5].

In bacteria, uptake of tungstate and molybdate, the oxidized form commonly found in the environment, involves multiple mechanisms, comprising a primary high-affinity ABC-type transporter, two secondary systems involving a low-affinity sulfate transporter and a non-specific anion transporter [6,7]. In *Escherichia coli* the high-affinity ABC transporter is encoded by three *mod* genes: ModA,[1] the soluble periplasmic protein responsible for high-affinity molybdate binding, ModB, the membrane pore forming protein, and ModC, the ATP-binding component responsible for energizing the transport reaction [8–11]. These *mod* genes are organized in two divergent operons encoding additional proteins such as ModE, a repressor DNA-binding protein, and a protein with an uncertain function (ModF) [6,12,13]. Although bacterial genes encoding molybdate transport proteins are typically present in a similar genetic and functional organization, only a few have been functionally and structurally characterized such as those of *Azotobacter vinelandii* [14], *Staphylococcus carnosus* [15], *Rhodobacter capsulatus* [16], *Anabaena variabilis* [17,18] and *Bradyrhizobium japonicum* [19].

* Corresponding author. Fax: +55 11 3091 7420.
E-mail address: abalan@usp.br (A. Balan).

[1] *Abbreviations used:* ModA, molybdate-binding protein; LB, Luria broth, CD, circular dochroism; XRF, X-ray fluorescence spectrometry.

1046-5928/$ - see front matter © 2006 Elsevier Inc. All rights reserved.
doi:10.1016/j.pep.2006.06.014

The ModA proteins share common characteristics with other ABC transporters binding proteins, including conformational changes following ligand binding and overall three-dimensional structure. These proteins encompass two similar globular domains, each composed by a central β-sheet flanked by α-helices connected by a hinge region formed by two interconnecting strands defining a deep cleft where the ligand binds by means of hydrogen bounds with uncharged polar groups of the protein [20,22]. In spite of these similar structural features, the amino acid sequences of known prokaryotic ModA proteins diverge quite significantly and differences in amino acid sequences may reflect altered ligand affinity according to the nutritional requirements of the different bacterial species [8].

The genus *Xanthomonas* includes a number of plant pathogens capable of infecting economically important host plants such as citrus, rice, beans, grapes, and cotton. *Xanthomonas axonopodis* pv. *citri* (*X. citri*) is one of the most economically relevant species, causing citrus canker affecting citrus cultivars around the world and inflicting economic losses estimated in hundreds of millions of dollars per year [23]. In this work, we describe the expression, purification and the biochemical analysis of the ModA protein, the putative periplasmic binding component of the molybdate uptake system in *X. citri*. The purification and biochemical characterization of the recombinant *X. citri* ModA ortholog is an important step toward definition of the three dimensional structure of this protein and will help in the understanding the role of molybdate transport in the physiology of this economically relevant phytopathogen.

Materials and methods

Bacterial strains and growth conditions

The *modA* gene was amplified from genomic DNA of the *X. citri* 306 strain [24]. All cloning steps were carried out using the *E. coli* DH5α strain while expression of the recombinant ModA protein was carried out with the *E. coli* BL21 (DE3) strain (Invitrogen). The recombinant strains were cultivated in Luria broth (LB) medium at 37 °C. Kanamycin (50 μg/mL) or ampicillin (100 μg/mL) was added to the growth medium in order to select cells transformed with pET28a or pGEM-T easy derivatives, respectively.

Plasmid construction

The nucleotide sequence of the *X. citri modA* gene, encoding the mature protein without the first 72 base pairs corresponding to an estimated 24 amino acid signal peptide, was amplified by PCR using a forward primer (5′ GT GCTGCATATGGCGCAGACCGCC 3′) and a reverse primer (5′ CGCCAAGCTTTCAATCCTTCAG 3′) with Platinum High Fidelity *Taq* polymerase (Invitrogen) based on standard amplification conditions. The forward primer included one *Nde*I restriction site, while the reverse primer encoded one *Hin*dIII restriction site (underlined primer sequences). The resulting amplified fragment, corresponding to 726 base pairs, was restricted with *Nde*I and *Hin*dIII enzymes (Invitrogen) and subsequently cloned into the expression vector pET28a (Novagen), previously digested with the same enzymes. Transformation efficiencies of approximately 10^8 cfu/μg DNA were routinely achieved with chemically competent *E. coli* DH5α cells. One recombinant colony, selected out of ten chosen colonies, was subjected to restriction analysis and nucleotide sequencing. The recombinant plasmid, named pETModA was further purified in larger quantities and transformed into the *E. coli* BL21 (DE3) strain (Novagen). One clone was selected for further analysis and submitted to an induction protocol with IPTG followed by cell lysis before purification of the recombinant protein. The *X. citri* ModA was expressed by the recombinant *E. coli* strain as a cytoplasmic protein with a His_6-tag genetically fused at the N-terminal end (HT-ModA).

Computational analysis

The nucleotide sequence of *modA* gene was obtained at NCBI (GI: 21109708). Search of ModA ortholog sequences was carried out using the KEGG2 program of the Bioinformatics Center Institute for Chemical Research, Kyoto University (www.genome.jp). The alignments of ModA amino acid sequences were obtained with the BLASTP program. Prediction of signal peptide and transmembrane sequences were determined with SignalP and DAS programs (http://www.cbs.dtu.dk/services/SignalP/ and http://www.sbc.su.se/~miklos/DAS/), respectively. Protein parameters of the *X. citri* ModA were calculated with programs available at the Expasy Molecular Biology Server (http://www.au.expasy.org/). Definition of conserved structural domains using the Conserved Domain Search (CDS) program available at NCBI (http://www.ncbi.nlm.nih.gov/Structure/cdd/wrpsb. cgi) was carried out as previously reported [25]. The PDB accession numbers for the *E. coli* bound to molybdate and tungstate and *A. vinelandii* orthologs are 1AMF, 1WOD and 1ATG, respectively. A molecular model of *Xac* ModA (Q8PHA1 code) based on the 1AMF structure was built using the Modbase entry (http://modbase.compbio.ucsf. edu).

Expression and purification of recombinant X. citri ModA protein

Cultures of the recombinant pETModA-transformed *E. coli* BL21 (DE3) strain were prepared aerobically in erlenmeyer flasks with LB or M9 medium supplemented with 50 μg/mL kanamycin until mid-log phase (OD_{600} 0.5–0.6) when IPTG was added to a final concentration of 0.1 mM. The cultures were induced aerobically (200 rpm) or statically for 2–4 h at 28 °C and 37 °C. Cells were collected by centrifugation at 8000*g* for 15 min at 4 °C and stored at −20 °C for approximately 16 h before lysis. The cell pellets

corresponding to 1 L of culture were suspended in 10 mL of Buffer 1 (50 mM sodium phosphate Buffer at pH 7.2 containing 100 mM NaCl, 5% glycerol and 5 mM imidazole) and incubated with lysozyme (final concentration of 100 μg/mL) for 1 h in an ice bath. Cells were sonically disrupted in a Branson Digital Sonifier (Model 450) and soluble fractions were separated from the non-soluble material by centrifugation at 16,000*g* for 20 min and 4 °C. The ModA protein was purified in batch from 15 mL of soluble fraction by immobilized metal affinity chromatography using nickel-charged resin from Invitrogen (Probond, according to manufacturer instructions). The charged resin was washed with Buffer 1 (10 bed volumes) followed by step gradient elution with buffers containing increasing concentrations of imidazole (20, 50, 100, 200 and 500 mM). Repurification of the flow-through was performed at the same way in order to increase the amount of purified protein. The fractions containing eluted protein were dialyzed 3 times for 6 h with 20 mM Tris–HCl at pH 8.2 containing 100 mM NaCl and then, further, concentrated with Ultrafree MWCO 5000 centrifugal filters (Amicon Millipore) to a final concentration of 20 mg/mL. Samples of 15 μL of the eluted protein fractions containing ~2 mg/mL were analyzed by SDS–PAGE using 12% acrylamide gels stained with Comassie Blue. Protein concentration was determined by spectrophotometer using the Edelhoch method [26].

Cleavage with thrombin and proteases

The *Xac* ModA purified protein was submitted to the cleavage with thrombin (2 mg/mL of protein and 1% of thrombin) during different times: 10 min, 20 min, 40 min, 1 h and 2 h. The proteases trypsin, chymotrypsin, papaine, subtilysin, and proteinase K also were used for attempts to cleave the His-tag at the same conditions. The reaction was stopped with 2 mM PMSF.

Fluorescence spectroscopy

Metal binding was followed by fluorescence measurements using an Aminco BOWMAN series 2 spectrofluorometer. Excitation and emission bandwidths were 4 and 8 nm, respectively. The fluorescence cell (1 × 1 cm) was mounted on a thermostatic holder. Tryptophan fluorescence was measured with an excitation wavelength of 295 nm and the emission spectra were recorded between 310 and 380 nm. All measurements were performed in 20 mM Tris–HCl pH 8.0 at 25 °C with the protein at concentration of 1.6 μM (40 μg/mL), calculated using the extinction coefficient for a molecular weight of 25.6 kDa. Sodium molybdate and tungstate were added to the protein solution and the emission spectrum recorded at the sensitivity range of the binding curve (0.1–10 μM). The fraction of metal–protein complex was determined by the increase of the intrinsic fluorescence. The measured fluorescence data were corrected for dilution and inner filter effects [27]. The corrected data were factored into a hyperbolic equation using non-linear least-square regression. Binding experiments were also carried out in the presence of saturating concentration of $NiSO_4$ (50 mM).

X-ray fluorescence spectrometry

All measurements were performed at the XRF beam line of the LNLS [28]. A white beam of 0.3 mm wide by 2 mm high was used to excite the samples under total reflection conditions. Samples were prepared as follows: 5 μL of a protein solution with a concentration of 2 mg/mL were dropped onto a Perspex support [29] and dried using a infrared lamp for 15 min. Samples were measured for 300 s and the X-ray spectra obtained were evaluated using the AXIL program [30].

Circular dichroism

Circular dichroism measurements were carried out with a JASCO J-810 spectropolarimeter equipped with a Peltier-type temperature controller and a thermostated cell holder, interfaced with a thermostatic bath. Spectra were recorded in 0.1 cm path length quartz cells at a protein concentration of 5 μM in 2 mM Tris–HCl buffer at pH 8.0 containing 50 mM NaCl in the absence or presence of 10 μM of Na_2MoO_4. Twenty consecutive scans were compiled and the average spectra stored. The data were corrected for the baseline contribution of the buffer and the observed ellipticities converted into the mean residue ellipticities [θ] based on a mean residue molecular mass of 101.2 Da. Thermal unfolding experiments were performed by increasing the temperature from 20 °C to 95 °C, allowing temperature equilibration for 5 min before recording each spectrum. The T_m represents the temperature at the midpoint of the unfolding transition. The secondary structure was estimated from fitted far-UV CD spectra using the CDNN software package [31].

Results

The X. citri mod operon and the ModA orthologs

The *Xanthomonas mod* genes are present in an operon-like organization similar to other bacterial species such as *Agrobacterium tumefasciens* and *Azotobacter vinelandii*. The *X. citri* and *X. campestris* ModA proteins share the highest amino acid sequence similarity (85% identity throughout the entire mature protein sequence) while lower similarity values were recorded with orthologs from other bacterial species such as *E. coli* K12 (45%) and *A. vinelandii* (23%). The *X. citri* ModA has 258 amino acids, including a putative signal peptide of 24 amino acids with a cleavage site located between Ala24 and Gln25. The predicted p*I* of the mature *X. citri* ModA protein is 9.5 and the amino acid composition consisted of 22.8% nonpolar, 39.61% uncharged polar, 15.3% acidic and 14.1% basic residues. The ModA proteins of *X. citri*

Table 1
Cultivation, induction conditions and recovery yields of both total and soluble recombinant *X. citri* ModA expressed by *E. coli* BL21 (DE3) cells

Induction temperature[a] (°C)	Aeration[b]	Culture media[c]	Induction period[d] (h)	Total protein[e] (g/L)	Soluble protein[f] (g/L)	% soluble protein[g]
37	+	LB	2	0.120	0.052	43.4
37	–	LB	4	0.110	0.064	58.2
37	+	M9	4	0.097	0.042	43.2
28	+	M9	4	0.126	0.073	58.0

[a] Incubation temperature following addition of inducer to the bacterial culture.
[b] Cultures kept in flasks within an orbital shaker set at 200 rpm (+) or kept statically (–) during the induction period.
[c] LB, Luria broth; M9, M9 minimal salt medium.
[d] Cultures were kept under inducing conditions for 2 h or 4 h.
[e] Total protein yields recovered from 1 L cultures kept in 3.6 L Fernbach flasks.
[f] Amounts of soluble protein purified after first metal affinity purification with nickel-charged resin and elution with imidazole-containing buffers.
[g] Amounts of soluble protein purified after first metal affinity purification expressed in percentage values of the total purified protein.

and *X. campestris* share the same amino acid number, molecular weight and p*I*. Analysis of functional domains carried out with the CDS program indicated that the *X. citri* and *X. campestris* ModA proteins are functionally and structurally conserved sharing the same identified domains.

Expression and purification of a recombinant X. citri ModA protein

The recombinant *X. citri* ModA protein was expressed and purified in *E. coli* BL21 (DE3) strain as a soluble cytosolic protein genetically fused at the N-terminal end with a His_6-tag and the thrombin cleavage site encoded by the pET28a expression vector. Previous attempts to express *X. citri* nutrient binding proteins in *E. coli* hosts revealed the relevance of culture conditions and induction protocols on the expression and solubility of the recombinant protein [32]. Four different induction protocols based on variation of temperature, aeration, culture media and induction time were tested in order to optimize the expression yields of both total and soluble recombinant protein (Table 1). Maximum soluble protein yields, representing up to 60% of the total expressed protein, were achieved after 4 h cultivation in LB medium at 37 °C with aeration. The recombinant protein with a calculated molecular weight of 25.6 kDa was purified by a single step affinity chromatography and eluted at different imidazole concentrations (Fig. 1). Approximately 65% of the recombinant protein was recovered at the end of the purification process and the protein remained soluble and stable at high concentrations (12–20 mg/mL), even after prolonged storage at −20 °C (two months). Re-purification of flow-through fractions increased the protein recovery yield in approximately 15% (data not shown). The total amount of protein did not change significantly at different culture conditions, except for a decrease of protein expression in cultures induced in M9 broth. Soluble *X. citri* ModA was recovered in all tested conditions but with better recovery rates for cultures prepared in LB with aeration. Attempts to remove the His_6-tag with different proteases, including thrombin, were unsuccessful in all conditions tested (data not shown).

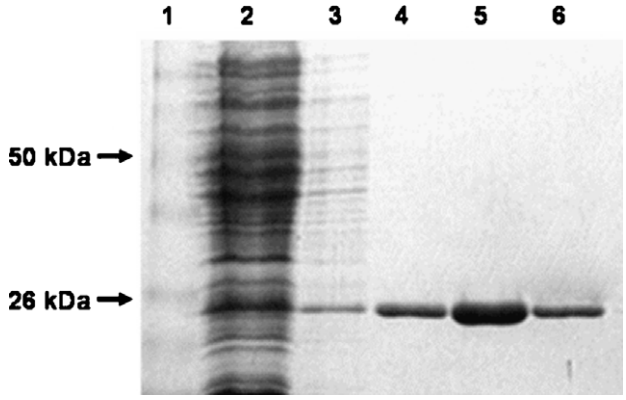

Fig. 1. Purification of the recombinant ModA protein by immobilized metal affinity chromatography after induction of *E. coli* BL21 (DE3) cells with IPTG. Protein samples were sorted in polyacrylamide gels and stained with Comassie blue. Lane 1, protein molecular weight markers; lane 2, flow-through of loaded nickel-containing resin (25 μg); lanes 3–6, aliquots (15 μL) of proteins eluted from the resin with 20, 50, 100 and 200 mM imidazole, respectively.

Fluorescence of ModA and characterization of the molybdate- and tunsgtate-binding activities

Fig. 2A shows the intrinsic tryptophan fluorescence spectrum of the recombinant *X. citri* ModA protein at pH 8.0. The maximum emission wavelength was centered at 336 nm with excitation at 295 nm. The rather long emission wavelength indicates that tryptophan residues of the protein are significantly exposed to the solvent. Addition of molybdate resulted in an increase (approximately 12% at saturation) of the intrinsic fluorescence emission of the protein. A similar increase in the intrinsic fluorescence emission was observed in the presence of tungstate (data not shown). Titration curves carried out with purified protein (1.6 μM) at pH 8.0 and molybdate or tungstate at concentrations ranging from 0.1 to 10 μM resulted in a hyperbolic curve saturating at concentrations over 2 μM, suggesting that the protein binds stoichiometric equivalent amounts of molybdate or tungstate (Fig. 2B). Based on these data, a K_d of 0.29 ± 0.1 μM for molybdate and 0.58 ± 0.14 μM for tungstate were determined for the recombinant *X. citri* ModA. The presence of a single molybdenum/tungsten-binding site

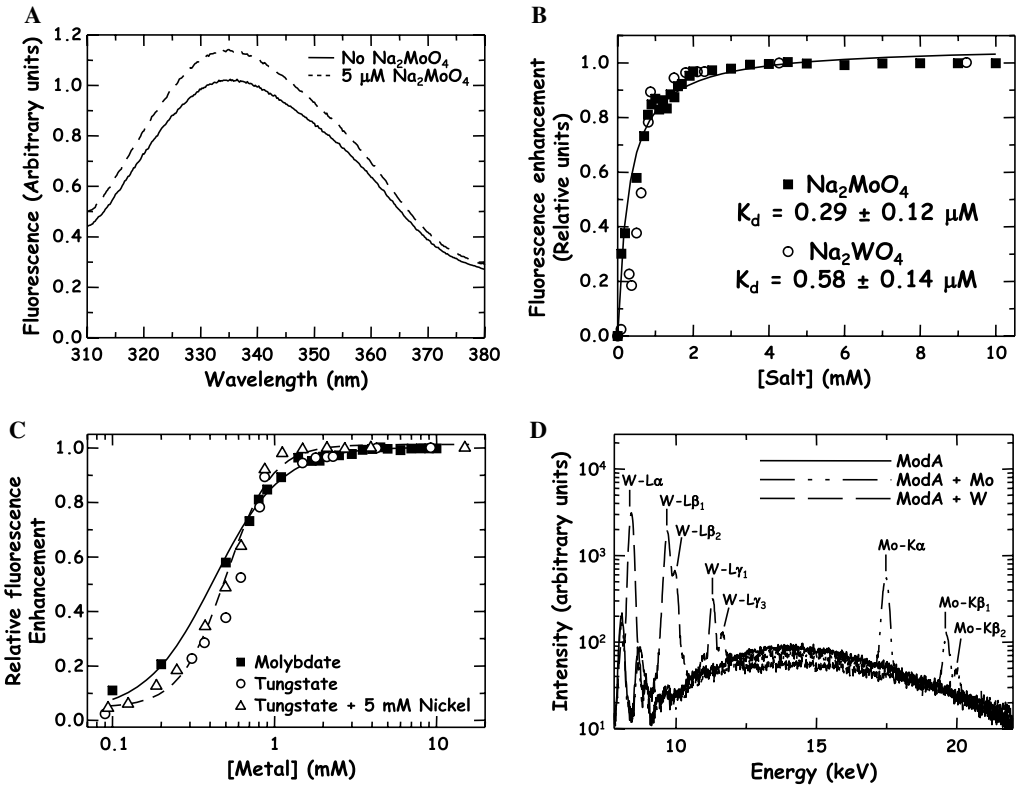

Fig. 2. Molybdate and tungstate-binding properties of the recombinant *X. citri* ModA protein. (A) ModA fluorescence emission spectra were recorded in the presence (dashed line) or absence of 5 mM Na_2MoO_4 (solid line). (B) Titration curves of ModA fluorescence after addition of molybdate (squares) or tungstate (circles) at concentrations ranging from 0.1 to 10 mM. Emission values were determined at 336 nm. Reported values represent the difference between the intrinsic fluorescence emission of apo-ModA and molybdate/tungstate titrated protein. The determined K_d values for molybdate and tungstate binding of the recombinant *X. citri* ModA are indicated. (C) Saturation curves of the recombinant ModA protein with molybdate and tungstate in the presence of $NiSO_4$. (D) Determination of X-ray fluorescence spectra of ModA bound to molybdate or tungstate. Samples were incubated with 5 μM sodium molybdate (black line), 5 μM sodium tungstate (clear gray lane) or without addition of anions (gray lane). The peaks represent the electro magnetic decaying for each element. All experiments were performed with 1.6 μM ModA in 20 mM Tris–HCl buffer at pH 8.0 and 25 °C.

at the *X. citri* ModA is in accordance with the determined structures of the *E. coli* and *A. vinelandii* orthologs [20,22]. The molybdate and tungstate binding affinities of the recombinant ModA were not affected by the presence of N-terminal His-tag since no significant changes in binding curves were detected in molybdate-binding experiments carried out with a saturating nickel concentration (50 mM) (Fig. 2C). Additionally no molybdate or tungstate traces were detected by X-ray fluorescence spectrometry in protein samples at concentrations up to 2-fold that used in the fluorescence experiments (Fig. 2D).

Molybdate-binding confers heat resistance and affects thermal unfolding transitions of X. citri ModA

The far-UV CD spectra of the *X. citri* ModA were recorded before and after addition of molybdate (Fig. 3A and B, curves of 20 °C). The spectra show a relative maximum at 192 nm and two relative minima at 208 and 222 nm. Analysis of the CD spectra confirmed that, similar to structurally defined orthologs, *X. citri* ModA belongs to the α/β type of binding proteins with a total content of 27% α-helices, 15% antiparallel and 9% of parallel β-sheet. Addition of 10 μM molybdate resulted in a small increase of the 208 nm spectrum indicating that the ligand binding results in a modest conformational change of the protein. As a consequence the estimated secondary structure content of the molybdate-bound ModA did not change significantly with regard to the unbound form of the protein. The small change of the ellipticity intensity of the band centered at 238 nm might more properly reflect the changed environment surrounding at least one of the tryptophan residues.

Binding of molybdate increased the thermal stability of the *X. citri* ModA protein by approximately 15 °C, as demonstrated in Figs. 3A and B. The measured T_m values for the unbound and molybdate-bound forms of the protein were 50.2 and 68.8 °C, respectively. The thermally induced unfolding was irreversible as inferred from the spectra obtained with samples submitted to different denaturing temperatures (70 and 95 °C) and subsequently cooled down. During the thermal unfolding of the protein the α-helical content was drastically reduced concomitantly with an increase of antiparallel β-sheet (see insets in Fig. 3). The thermal unfolding of the protein also results in protein precipitation detected at completion of the experiment, either in the absence or presence of sodium molybdate.

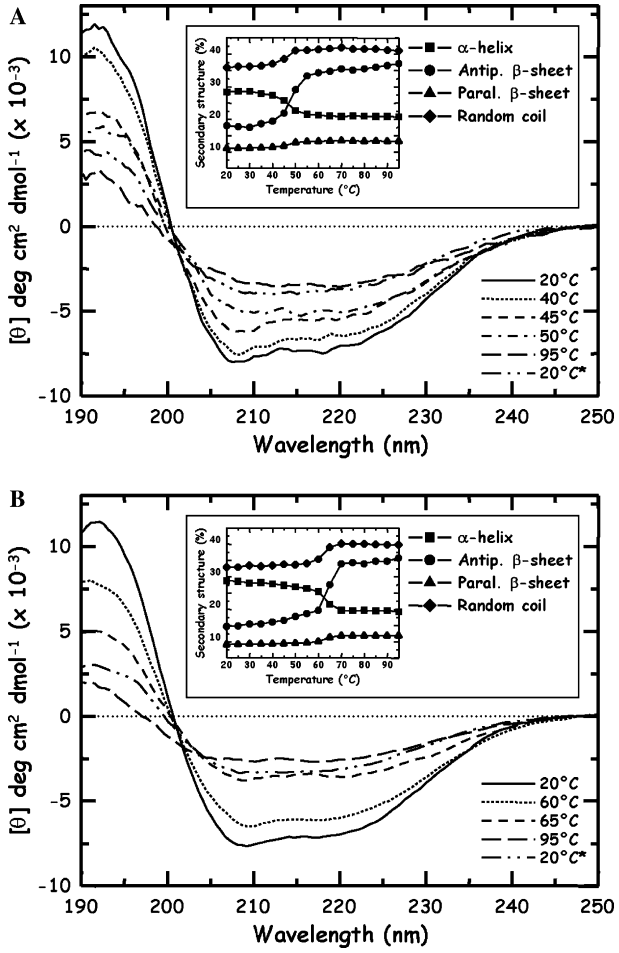

Fig. 3. Temperature-dependent denaturation of the recombinant *X. citri* ModA in the absence (A) or presence (B) of 10 μM sodium molybdate. The far-UV CD spectra were recorded using 5 μM of purified ModA in 2 mM Tris–HCl buffer at pH 8.0 containing 50 mM NaCl at the indicated temperatures. One sample (20 °C*) was incubated at 20 °C after previous heating at 95 °C. The insets show the changes in the secondary structure of ModA at different incubation temperatures in the absence (A) or presence (B) of molybdate.

Discussion

Molybdenum uptake is a vital step in the nitrogen metabolism of several bacterial species, however, no information concerning the presence, function and structural characteristics of the molybdenum transport components is present available for *Xanthomonas* species, which usually thrive both as plant pathogens and soil inhabitants. In this work we identified and characterized the soluble molybdenum-binding component of the putative Mod uptake system of *X. citri*. The *X. citri* ModA was successfully purified from a recombinant *E. coli* strain without detectable endogenous bound molybdate and remained proficient in the binding of both molybdate and tungstate. Binding of molybdate conferred a significant thermal stability to the recombinant protein indicating that ligand-binding activity reflects an endogenous feature of the protein. These evidences indicate that the recombinant ModA preserved both functional and structural features of the native *X. citri* protein.

The *mod* operon, encompassing the *modA*, *modB* and *modC* genes, was found as a single polycistronic unit in the genomes of both *X. citri* and *X. campestris*. Comparison of the bacterial ModA amino acid sequences revealed that the *X. citri* ortholog is closely related to the protein encoded by *X. campestris*. Indeed, the amino acid sequences of mature ModA proteins expressed by *X. citri* and *X. campestris* orthologs show an overall identity of 85%. The *X. citri* ModA shares also rather high similarity values with the *E. coli* and, to a lesser extent, with the *A. vinelandii* orthologs, which have experimentally defined three-dimensional structures [20,22]. All seven amino acids, including the four NH groups of the main chain (Ser12, Ser39, Ala125, Val152) and three side OH chains (Ser12, Ser39, and Tyr170), participating in the formation of hydrogen bonds involved in molybdate/tungstate binding are conserved between the *E. coli* and *X. citri* orthologs suggesting that these proteins are functionally and structurally conserved. In fact, a previous analysis of *Xac* ModA molecular modeling generated by the Modbase entry revealed that both proteins, *E. coli* and *Xac* ModA, share 52% of identity and have similar structures.

In order to obtain sufficient protein for functional and structural studies, the *X. citri* ModA protein was expressed and purified from a recombinant *E. coli* strain. The recombinant protein was expressed in *E. coli* as a soluble intracellular protein genetically fused at the N-terminal end with an additional sequence encompassing the His_6-tag employed in the single step affinity chromatography purification. Attempts to express the recombinant *X. citri* with an intact signal peptide and a C-terminal His_6-tag failed to promote secretion to the periplasmic space of the recombinant strain suggesting that the secretion apparatus of *E. coli* does not efficiently recognize the signal sequence of ModA, as well as other periplasmic binding proteins [32]. Successful expression and high recovery yields of soluble *X. citri* ModA was achieved only after removing the putative signal peptide and fusion of the His_6-tag at the N-terminal region. The re-purification procedure also was an important step for the acquisition of sufficient amounts of protein for the crystallization assays and subsequent structural analysis of *X. citri* ModA protein [33].

The recombinant *X. citri* ModA protein binds stoichiometrically equivalent amounts of molybdate and tungstate with K_d values of 0.29 ± 0.12 μM and 0.58 ± 0.14 μM, respectively. The molybdate-binding affinity of the *X. citri* ModA is within the range of the previously reported *E. coli* ortholog [34] and other cytoplasmic molybdate-binding proteins such as *Haemophilus influenzae* Mop (<1 μM) [35] and *E. coli* ModE (0.8 μM) [36], adding a further evidence that the recombinant protein preserved the endogenous anion-binding activity of the native *X. citri* protein.

One serious concern regarding the biochemical characterization of the *X. citri* ModA was the presence of a N-terminal His_6-tag that could not be proteolytically removed

from the recombinant protein. X-ray fluorescence spectrometry determinations showed that the purified recombinant protein was molybdate and tungstate-free, thus, indicating that the measured anion-binding affinities reflects an endogenous property of the protein. Additionally, experiments carried out in the presence of saturating nickel concentrations indicated that the His_6-tag did not interfere with the molybdate binding properties of the recombinant protein.

The intrinsic fluorescence spectra displayed by the *X. citri* ModA protein after addition of molybdate indicate a hyperfluorescence phenomenum. According to the three dimensional structures defined for the *E. coli* and *A. vinelandii* orthologs, no significant conformational changes occur after molybdate binding, thus suggesting that the altered spectroscopy spectra observed after ligand binding more properly reflect small alterations of the environment surrounding the tryptophan residues. In fact, circular dichroism analysis of the protein in the presence or absence of the molybdate did not reveal significant alterations in the content of secondary structures. These evidences indicate that the recombinant protein preserves active features, thus, supporting its use for the definition of the three dimensional structure of the *X. citri* ModA protein.

The binding of molybdate to the *X. citri* ModA conferred a remarkable thermal stability to the ModA since the T_m of the recombinant protein was enhanced from approximately 50 °C, in the unbound state, to 65.8 °C in the presence of molybdate. Similar to other ABC-type transporters ligand components, the basic structural design of the *E. coli* and *A. vinelandii* ModA protein consists of two similar domains separated by a deep cleft [21,22,37]. The binding of molybdate to bacterial ModA involves the formation of seven hydrogen bonds with uncharged polar amino acid groups located at the amino-terminal ends of four α-helices. Indeed, the anion charge is stabilized by highly localized dipoles at the helices termini without the interplay of positively charged residues at the termini of the binding helices [21]. A similar structure is also present in the *X. citri* ModA (40% of sequence identity with *E. coli* ortholog), thus indicating that the enhanced thermal stability of the protein is a consequence of the role of molybdate in the protein structure in which key amino acids facing the binding cleft help to keep the protein in a more compact and stable conformation. These data corroborate the fact that crystals of *X. citri* ModA only were obtained in the presence of molybdate [33], probably because the bound protein assumes a more stable conformation. The irreversible thermal denaturation of *X. citri* ModA was characterized by the increase of β-sheet and random coil content and the concomitant decrease of the α-helices, leading to aggregation and precipitation of the protein, which hampered the use of the protein in thermodynamic studies.

Although *Xanthomonas* species are not nitrogen fixing bacteria, the presence of the *mod* operon in the genome of two recently sequenced species (*X. citri* and *X. campestris*) is intriguing. A sequence search indicated that enzymes requiring molybdenum-containing cofactors, such as nitrate reductase or nitrogenase, are not present in the genome of *X. citri* but are preserved in *X. campestris*. Curiously, *X. citri*, but not *X. campestris*, carries an *opp* operon encoding an ABC transporter dedicated to the uptake of oligopeptides, an alternative nitrogen sources [38]. Thus, it is conceivable that *Xanthomonas* species have evolved different physiological strategies to obtain nitrogen from the environment and molybdenum uptake may have distinct physiological relevance for *X. citri* and *X. campestris*. Additional studies involving the isolation and characterization of specific knockout mutants aiming the elucidation of the physiological role of molybdenum are under way and will certainly contribute to a better understanding of the *X. citri* and *X. campestris* Mod systems.

Acknowledgments

This work was supported by a FAPESP grant as part of the Program of Structural and Molecular Biology Network (SMolBNet). We thankfully acknowledge the continuous incentive and support of Dr. Rogério Meneghini, leader of the SMolBNet program. We also thank S.S. Lucas for the helpful technical support and J. Hesson for reviewing the manuscript.

References

[1] R.J.P. Williams, J.J.R. Fraústo da Silva, The involvement of molybdenum in life, Biochem. Biophys. Res. Commun. 292 (2002) 293–299.
[2] R.N. Pau, D.M. Lawson, Transport, homeostasis, regulation, and binding of molybdate and tungstate to proteins, Met. Ions Biol. Syst. 39 (2002) 31–74.
[3] K.V. Rajagopalan, J.L. Johnson, The pterin molybdenum cofactors, J. Biol. Chem. 267 (1992) 10199–10202.
[4] C. Kisker, H. Schindelin, D.C. Rees, Molybdenum-cofactor-containing enzymes: Structure and Mechanism, Ann. Rev. Biochem. 66 (1997) 233–267.
[5] A. Kletzin, W.W. Adams, Tungsten in biological systems, FEMS Microbiol. Rev. 18 (1996) 5–63.
[6] A.M. Grunden, K.T. Shanmugam, Molybdate transport and regulation in bacteria, Arch. Microbiol. 168 (1997) 345–354.
[7] W.T. Self, A.M. Grunden, A. Hasona, K.T. Shanmugam, Molybdate transport, Res. Microbiol. 152 (2001) 311–321.
[8] S. Johann, S.M. Hinton, Cloning and nucleotide sequence of the *chlD* locus, J. Bacteriol. 169 (1987) 1911–1916.
[9] S. Rech, U. Deppenmeier, R.P. Gunsalus, Regulation of the molybdate transport operon, *modABCD*, of *Escherichia coli* in response to molybdate availability, J. Bacteriol. 177 (1995) 1023–1029.
[10] J.A. Maupin-Furlow, J. Rosenthel, J.H. Lee, U. Deppenmeier, R.P. Gunsalus, K.T. Shanmugan, Genetic analysis of the *modABCD* (molybdate transport) operon of *Escherichia coli*, J. Bacteriol. 177 (1995) 4851–4856.
[11] S. Rech, C. Wolin, R.P. Gunsalus, Properties of the Periplasmic ModA Molybdate-binding protein of *Escherichia coli*, J. Biol. Chem. 271 (1996) 2557–2562.
[12] G.L. Corcuera, M. Bastidas, M. Dubourdieu, Molybdenum uptake in *Escherichia coli* K12, J. Gen. Microbiol. 139 (1993) 869–1875.
[13] A.M. Grunden, W.T. Self, M. Villain, J.E. Blalock, K.T. Shanmugam, An analysis of the binding of repressor protein ModE to *modABCD* (molybdate transport) operator/promoter DNA of *Escherichia coli*, J. Biol. Chem. 274 (1999) 24308–24315.

[14] F. Luque, L.A. Mitchenall, M. Chapman, R. Cristine, R.N. Pau, Characterization of genes involved in molybdenium transport in *Azotobacter vinelandi*, Mol. Microbiol. 7 (1993) 457–459.
[15] H. Neubauer, I. Pantel, P.E. Lindgren, F. Gotz, Characterization of the molybdate transport system ModABC of *Staphylococus carnosus*, Arch. Microbiol. 172 (1999) 109–115.
[16] G. Wang, S. Angermuller, W. Klipp, Characterization of the *Rhodobacter capsulatus* genes encoding a molybdenum transport system and putative molybdenum–pterin-binding proteins, J. Bacteriol. 175 (1993) 3031–3042.
[17] T. Thiel, B. Pratte, M. Zabalak, Transport of molybdate in the cyanobacterium *Anabaena variabilis* ATCC 29413, Arch. Microbiol. 179 (2002) 50–56.
[18] M. Zahalak, B. Pratte, K.J. Werth, T. Thiel, Molybdate transport and its effect on nitrogen utilization in the cyanobacterium *Anabaena variabilis* ATCC 29419, Mol. Microbiol. 51 (2004) 539–549.
[19] M.J. Delgado, A. Tresierra-Ayala, C. Talbi, E.J. Bedmar, Functional characterization of the *Bradyrizobium japonicum modA* and *modB* genes involved in molybdenum transport, Microbiology 152 (2006) 199–207.
[20] Y. Hu, S. Rech, R.P. Gunsalus, D.C. Rees, Crystal structure of molybdate-binding protein ModA, Nat. Struct. Biol. 4 (1997) 703–707.
[21] D.M. Lawson, C.E. Williams, D.J. White, A.P. Choay, L.A. Mitchenall, R.N. Pau, Proteins ligand for molybdate, specificity and charge stabilization at the anion-binding sites of periplasmic and intracellular molybdate-binding proteins of *Azotobacter vinelandii*, J. Chem. Soc., Dalton Trans. 21 (1997) 3981–3984.
[22] D.M. Lawson, C.E. Williams, L.A. Mitchenall, R.N. Pau, Ligand-size is the major determinant of specificity in periplasmic oxyanion-binding proteins: the 1.2 Å resolution crystal structure of *Azotobacter vinelandii* ModA, Struct. Fold. Des. 6 (1998) 1529–1539.
[23] A.M. Brunings, D.W. Gabriel, *Xanthomonas citri*: breaking the surface, Mol. Plant Pathol. 4 (2003) 141–147.
[24] A.C. da Silva, J.A. Ferro, F.C. Reinach, C.S. Farah, L.R. Furlan, et al., Comparison of the genomes of two *Xanthomonas* pathogens with differing host specificities, Nature 417 (2002) 459–463.
[25] A. Marchler-Bauer, S.H. Bryant, CD-search: protein domain annotations on the fly, Nucleic Acids Res. 32 (2004) 327–331.
[26] H. Edelhoch, Spectroscopic determination of tryptophan and tyrosine in proteins, Biochemistry 6 (1967) 1948–1954.
[27] M.L. Mertens, J.H.R. Kägi, A graphical correction procedure for inner filter effect in fluorescence quenching titrations, Anal. Biochem. 96 (1979) 448–455.
[28] C.A. Pérez, M. Radtke, H.J. Sánchez, H. Tolentino, R.T. Neuenshwander, W. Barg, M. Rubio, M.I.S. Bueno, I.M. Raimundo, J.J.R. Rohwedder, Synchrotron radiation X-ray fluorescence at the LNLS: beamline instrumentation and experiments, X-ray Spectrom. 28 (1999) 320–326.
[29] M. Schmitt, P. Hoffmann, K.H. Lieser, Perspex as sample carrier in TXRF, Fresenius Z. Anal. Chem. 328 (1987) 594–595.
[30] B. Vekemans, K. Janssens, L. Vincze, F. Adams, P.E. Vanspen, Analysis of X-ray spectra by interative least squares (AXIL): new developments, X-ray Spectrom. 23 (1994) 278–285.
[31] G. Bohm, R. Murh, R. Jaenicke, Quantitative analysis of protein far UV circular dichroism spectra by neural networks, Protein Eng. 5 (1992) 191–195.
[32] A. Balan, C.S. Souza, A. Moutran, R.C.C. Ferreira, C.S. Franco, C. Ramos, L.C.S. Ferreira, Purification and *in vitro* characterization of the maltose-binding protein of the plant pathogen *Xanthomonas citri*, Protein Exp. Purif. 43 (2005) 103–110.
[33] C.P. Santacruz, A. Balan, L.C.S. Ferreira, J.A. Barbosa, Crystallization, data collection and phasing of the molybdate-binding protein of the phytopathogen *Xanthomonas axonopodis* pv. *citri*, Acta Crystallogr. Sect. F. Struct. Biol. Crystal. Commun. 62 (2006) 289–291.
[34] J. Imperial, M. Hadi, N.K. Amy, Molybdate binding by ModA, the periplasmic component of the *Escherichia coli mod* molybdate transport system, Biochem. Biophys. Acta 1370 (1998) 337–346.
[35] A.K. Duhme, W. Meyer-Klaucke, D.J. White, L. Delarbre, L.A. Mitchenall, R.N. Pau, Extended X-ray absorption fine structure studies on periplasmic and intracellular molybnedum-binding proteins, J. Biol. Inorg. Chem. 4 (1999) 588.
[36] L.A. Anderson, T. Palmer, N.C. Price, S. Borneman, D.H. Boxer, R.N. Pau, Characterisation of the molybdenum-responsive ModE regulatory protein and its binding to the promoter region of the *modABCD* (molybdenum transport) operon of *Escherichia coli*, Eur. J. Biochem. 246 (1997) 119–126.
[37] M.A. Dwyer, H. Hellinga, Periplasmic binding proteins: a versatile superfamily for protein engineering, Curr. Opin. Struct. Biol. 14 (2004) 495–504.
[38] A. Moutran, R.B. Quaggio, A. Balan, L.C.S. Ferreira, R.C.C. Ferreira, The oligopeptide permease (Opp) of the plant pathogen *Xanthomonas axonopodis* pv. *citri*, Curr. Microbiol. 48 (2004) 354–359.